20
Structural Properties and Applications of Self-Assembling Peptides

Zhongli Luo and Shuguang Zhang

20.1
Introduction to Self-Assembling Peptides

Q1 In 1993, one• of us (Shuguang Zhang) reported that a short peptide segment called *EAK16* from the yeast protein *Zuotin* [1] could undergo self-assembly to form scaffolds visible to the naked eye which were similar to amyloid deposits in terms of β-sheet structure and fibrillar architecture [2]. We have subsequently expanded designer self-assembling peptide materials using the 20 natural L-amino acids and some D-amino acids. Applications include (i) 3D tissue cell cultures, (ii) cell and tissue engineering, (iii) controlled drug delivery and regenerative medicine, and (iv) trauma emergency. This chapter focuses on self-assembling peptides with regards to principles of design, structural transitions, and diverse applications.

20.2
The Principles of Self-Assembling Peptides

20.2.1
Design Principle for Self-Assembling Peptides

Molecular self-assembly, that is, the spontaneous association of molecular components into well-organized structures, is a finely tuned balance between numerous non-covalent weak interactions. For self-assembling peptides, key elements are chemical complementarities and structural compatibility through numerous non-covalent weak interactions [3]. These include: (i) hydrogen bonds, (ii) electrostatic interactions, (iii) hydrophobic interactions, (iv) van der Waals force, and (v) water-mediated hydrogen bonds [3]. Each interaction in isolation is rather weak, but collectively they exert strong molecular forces to facilitate formation of molecular structures and to maintain the stability of these structures, allowing them to be harnessed in the design of simple self-assembling peptides. Such peptides generally show a simple pattern of hydrophilic and hydrophobic residues in the primary

Amyloid Fibrils and Prefibrillar Aggregates, First Edition. Edited by Daniel Erik Otzen.

Color Fig.: **20.1**

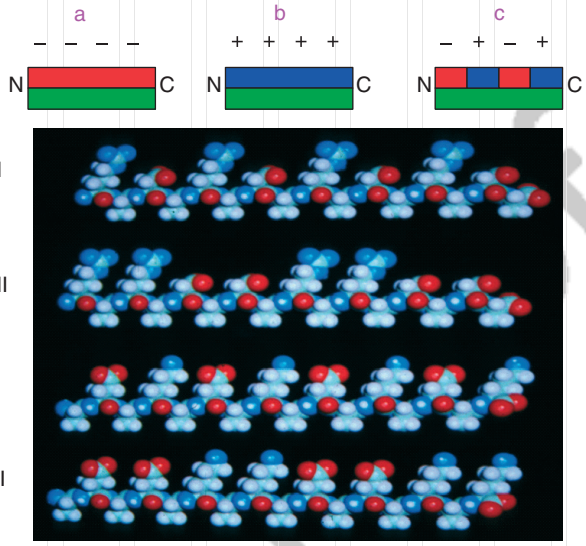

Figure 20.1 Schematic and molecular models of the designer amphiphilic self-assembling peptides which form well-ordered nanofibers (sequences provided in Table 20.1). (a) These peptides have two distinctive sides, one hydrophobic, and the other hydrophilic. The hydrophobic side forms a double sheet inside the fiber and the hydrophilic side forms the outside of the nanofibers that interact with water molecules, forming a hydrogel with up to 99.9% water. At least three types of molecules can be made, with −, + or −/+ on the hydrophilic side. (b) The individual self-assembling peptide molecules are ∼6 nm long. The first such peptide, EAK16-II, was discovered from a yeast protein, zuotin [2]. This peptide has inspired us to design a large class of self-assembling peptide construction motifs. When dissolved in water in the presence of salt, they spontaneously assemble into well-ordered nanofibers and then further into scaffolds [2, 4, 5]. (Reproduced from Refs. [2, 4, 5] with permission.)

sequences (Figure 20.1a), furthermore, the content of hydrophobic features and the distinction between polar and non-polar surfaces generally plays an important role in the design, synthesis and production of self-assembling peptides (Figure 20.1b).

The self-assembling peptides family can be expanded while containing the same charge distribution by the use of different amino acids, for example, EAK → DAR. These peptides contain a systematic arrangement of negatively and positively charged residues that utilize electrostatic interactions, hydrogen bonds, and van der Waal's forces to control molecular self-assembly. For example, the simplest and most widely studied self-assembling peptides contain three types of charge patterns [2, 4, 6], type I, − +; type II, − − + +; type IV, − − − − + + + + (Figure 20.1a, Table 20.1). This classification is based on the hydrophilic surface of the molecules that have alternating + and − charged amino acid residues, alternating in groups of 1, 2, 3, 4, and so on. These well-defined sequences allow them to undergo ordered self-assembly, resembling well-studied polymer assemblies. In addition,

Table 20.1 Sequences of self-assembling peptides.

Name[a]	Sequence	Ionic modulus[b]	Structure[c]	Direct conversion[d]	Matrix formation[e]
EAK12-a	—	II	r.c	No	No
EAK12-b	$\overset{+}{A}K\overset{-}{A}S\overset{-}{A}E\overset{+}{A}\overset{-}{A}K\overset{+}{A}K$	II	r.c	No	No
EAK12-c	$\overset{+}{A}K\overset{-}{A}E\overset{-}{A}E\overset{-}{A}E\overset{+}{A}\overset{-}{A}K\overset{+}{A}K$	I/II	r.c	No	No
EAK12-d	$\overset{-}{A}E\overset{-}{A}E\overset{-}{A}E\overset{-}{A}E\overset{+}{A}K\overset{+}{A}K$	IV/II	α/β	Yes	Yes
DAR16-IV	$n-\overset{-}{A}D\overset{-}{A}D\overset{-}{A}D\overset{-}{A}D\overset{+}{A}R\overset{+}{A}R\overset{+}{A}R\overset{+}{A}R$	IV	α/β	Yes	Yes
DAR16-IV*	$n-\overset{-}{D}A\overset{-}{D}A\overset{-}{D}A\overset{-}{D}A\overset{+}{R}A\overset{+}{R}A\overset{+}{R}A\overset{+}{R}A$	IV	α/β	Yes	Yes
RADA16-I	$\overset{+}{R}A\overset{-}{D}A\overset{+}{R}A\overset{-}{D}A\overset{+}{R}A\overset{-}{D}A\overset{+}{R}A\overset{-}{D}A$	I	β	No	Yes
RADA16-IV	$\overset{+}{R}A\overset{+}{R}A\overset{+}{R}A\overset{+}{R}A\overset{-}{D}A\overset{-}{D}A\overset{-}{D}A\overset{-}{D}A$	IV	β	No	Yes

[a] The number following each name indicates the chain length of the oligopeptides. N- and C-termini of the oligopeptides are acetylated and amidated, respectively.
[b] Type I, ''molecular Lego'' forms a hydrogel scaffold for tissue engineering; Type II, ''molecular switch'' as a molecular actuator; Type III, ''molecular hook'' and ''molecular velcro'' for surface engineering (not populated by the peptides in this Table); Type IV, − − − − + + + +peptide nanotubes and nanovesicles, or ''molecular capsule'' for protein and gene deliveries.
[c] ®, β sheet; α-helix; r.c., random coil.
[d] Direct conversion to self-assembled structures occurs when there is no detectable intermediate by CD spectroscopy.
[e] Matrix formation means that the peptide forms a macroscopic hydrogel matrix with nanofiber structures upon exposure to saline conditions [2–4, 6, 11].

alternating hydrophobic and hydrophilic residues, or a distinct periodicity of polar and non-polar in sequence or mixed together [7, 8], is one of the important criteria in designing self-assembling peptides (Figure 20.1b) [2, 9, 10]. Application of these simple and clear principles to the 20 natural L-amino acids leads to the design of a wide range of self-assembling peptides (Table 20.1).

20.2.2 Conformational Changes Undergone by Self-Assembling Peptides

Depending on the environment and the peptide sequence, self-assembling peptides can switch from α-helix to β-sheet or vice versa [12, 13]. Environmental factors include temperature, pH, peptide concentration, ionic strength, and buffer composition, as detailed in the following.

20.2.2.1 Effect of Temperature

Most self-assembling peptides are stable as monomers in one structural state at ambient-to-physiological temperatures [3]. However, some L-amino acid peptides

Color Fig.: **20.2**

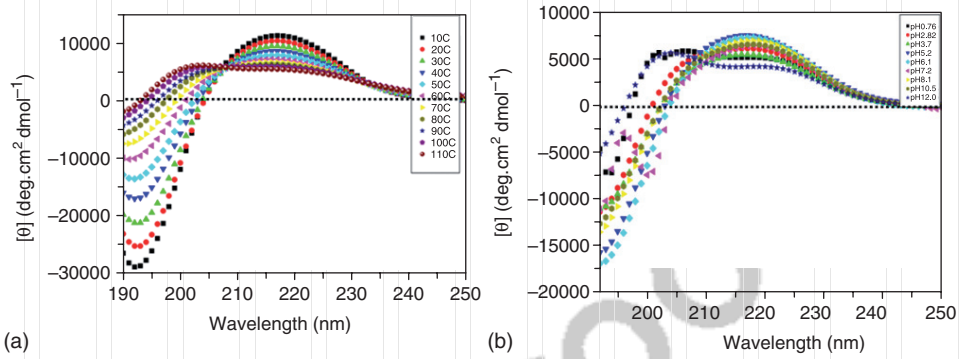

Figure 20.2 The effects of temperature and pH values of the D-form peptide d-EAK16. (a) The CD spectra of d-EAK16 from 10 to 110 °C. (b) CD spectra undergo significant variation between pH 0.7 and 12.0. (Reproduced from Ref. [15] with permission.)

like EAK12-d and DAR16-IV* undergo an abrupt structural transition from β-sheet to α-helix at higher temperatures [14]. The β-sheet structure of the D-amino acid peptide d-EAK16 is relatively stable up to 70 °C (Figure 20.2a) [15] but switches from β-sheet to a more α-helix-rich but still monomeric state above 80 °C in a two-state transition similar to l-EAK12 and l-DAR16-IV*. There is no significant self-assembly at this time scale [16].

20.2.2.2 Effect of pH

It is well known that pH changes have drastic effects on protein and peptide structures [17]. EAK12-d and DAR16-IV* can also undergo conformational changes as a function of pH. At pH values of 0.8 and 12.0, d-EAK16 shows a characteristic α-helical spectrum, while it is more β-sheet rich between pH 3.7 and 7.0 (Figure 20.2b). The β-amyloid peptide Aβ (A1–42) shows similar pH dependence, forming α-helical structures at pH 1.3 and 8.3 and β-sheet around pH 5.4 [18].

20.2.2.3 Effect of Amino Acid Sequence

Since α-helices have 3.6 amino acid residues per turn, separating two amino acids that interact strongly by 4 amino acids (i.e., i, $i + 4$) may increase the stability of the α-helix [19]. Marqusee and Baldwin showed that the peptide with K and E at the (i, $i + 4$) positions had a high helix stability over the pH-range 2–12 [20]. In general, amino acid sequence and ionic complementarities contribute to the overall propensity to form a specific secondary structure, as well as to the stability of the secondary structure.

A given amino acid sequence can undergo significant changes if different combinations of D- and L-amino acids are employed [21]. Figure 20.3 shows this for the following four peptides: (i) all D-amino acids in d-EAK16, (ii) all L-amino acids in l-EAK16, (iii) EA*K16 sequence (only A* is a D-amino acid), and (iv) E*AK*16 (all except Ala are D-amino acids).

Color Fig.: **20.3**

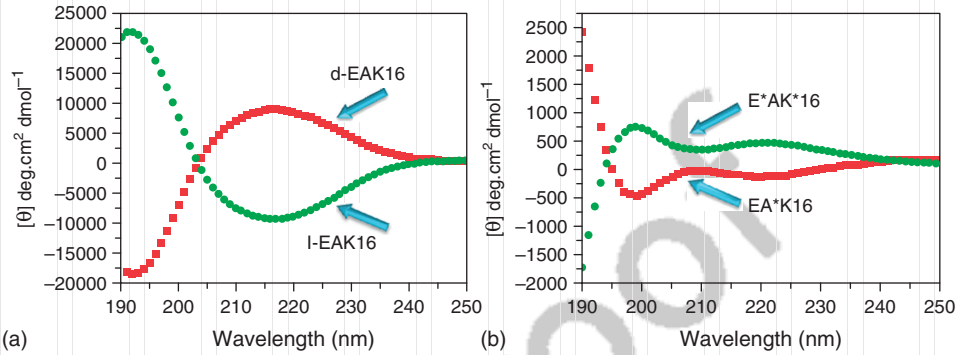

Figure 20.3 CD spectra of four different peptides at 37 °C. See text and Table 20.1 for sequence details. Note the pairwise inverted CD spectra reflecting differences in chirality. (Reproduced from Ref. [21] with permission.)

The circular dichroism (CD) spectrum of d-EAK16 is the mirror image of l-EAK16, its enantiomer. However, the peptide E*AK*16, which is a diastereomer of l-EAK16, has a minimal ellipticity at 208 nm and a maximal ellipticity at 199 nm, which is neither a typical β-sheet nor an α-helix formation, but closer to "random coil" CD spectra. The mixed chiral amino acids in the peptides indeed drastically alter the secondary structures, especially for the D-amino acid substitutions that disrupt the β-sheet structure in either all L- or all D-form peptides, compromising its self-assembly properties [21] (Figure 20.3).

The link between secondary structure changes and the process of self-assembly is discussed in Section 20.3.2.

20.3 Self-Assembling Peptide Nanofibers

20.3.1 The Nanofiber Structures of the Peptide Scaffold

Scanning electron microscopy, atomic force microscopy, and transmission electron microscopy reveal some self-assembling peptides fibers to be ~10–20 nm in diameter [2, 4, 22] (Figure 20.4a). Nanofiber network and pores (between nanofibers, with diameters ranging from 50 to 200 nm, Figure 20.4b) are similar to those found with biologically derived substrates such as the extracellular matrix (ECM). Because the fiber density correlates with the peptide concentration, we always use a high peptide concentration (~1%, w/w) to produce high-density nanofibers for the 3D scaffold. Some nanofibers resist protease degradation by proteases, including trypsin, α-chymotrypsin, papain, protease K, and pronase [22].

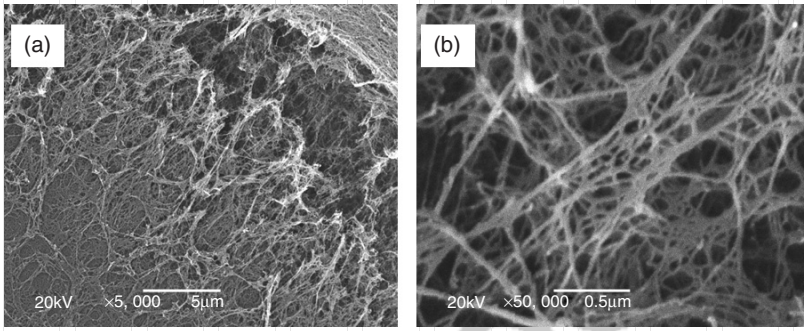

Figure 20.4 SEM serial photograph of d-EAK16. The diameter of the nanofibers is about 10 nm, and the pores are about 20–500 nm. (a) 5000× and (b) 50 000× magnifications. The nanofiber structure of d-EAK16 is similar to that of L-EAK16. The diameter of the nanofibers of l-EAK16 is ∼10 nm, and the pores of the scaffold are about 20–500 nm. (Reproduced from Ref. [22] with permission.)

20.3.2 The Process of Peptide Scaffold Formation

Self-assembly of d-EAK16 nanofibers may be followed by AFM [21]. At $t = 0$ (immediately after sonication), irregular particles are observed. At ∼4 h, many short nanofibers appear; 10 h later, most of them have self-assembled into ∼200 nm nanofibers. At ∼12 h, these short fibers have lengthened and self-assembled further into longer nanofibers and some of them appear to connect to each other. At ∼16 h a majority of nanofibers form a 3D scaffold network. At ∼24 h, d-EAK16 have self-assembled into a 3D nanofibers scaffold with a nanoscale structure like multilayered fishing nets (Figure 20.5a). d-EAK16 undergoes dynamic self-assembly to form a well-ordered nanofiber scaffold in pure water, but salts significantly accelerate the process [21, 22]. d-EAK16 can self-assemble to nanofibers induced by physiological salt concentrations at room temperature. Incubation at 100 °C for 4 h leads to a structural transition from β-sheet to α-helix. Addition of phosphate-buffered saline solution (PBS) to the peptide solution and overnight incubation leads to nanofibers. After continuous incubation for two days, almost all peptides formed nanofibers. The results suggest that d-EAK16 undergoes a secondary structure transition, but it still can form nanofibers and its quaternary structure is little affected by temperature (Figure 20.5a–c) [15]. d-EAK16 can still self-assemble to nanofibers in the presence of various denaturation agents such as 1% SDS, or 8.1 M urea or 7.1 M guanidine.HCl (Figure 20.5d–f).

Another test is to use sonication to break RADA16-I nanofibers (Figure 20.6) [16]. Sonicated fragments not only quickly reassemble into nanofibers that are indistinguishable from the original nanofibers, but their reassembly also leads to increased scaffold rigidity according to rheological analyses.

Color Fig.: **20.5**

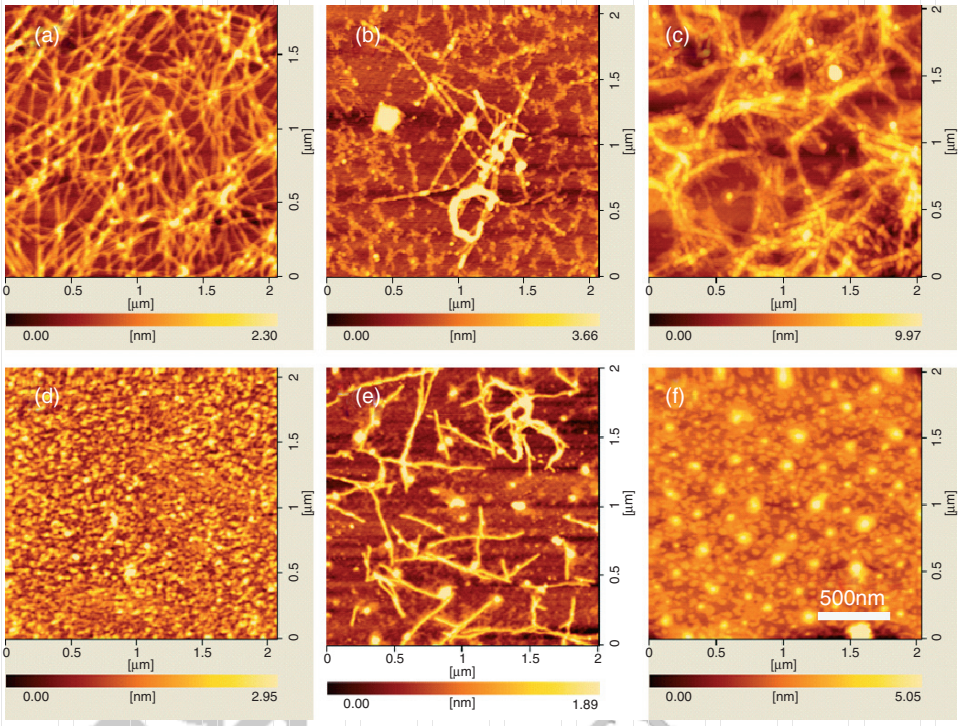

Figure 20.5 AFM images of d-EAK16 (1 mg ml^{-1}, 0.1%) under repeated cycles of thermal treatment at different pH values. (a) d-EAK16 solution was incubated at 25 °C for 4 h, and then PBS was added to induce self-assembly overnight. (b) d-EAK16 solution was incubated at 100 °C for 4 h, and PBS was added to induce self-assembly overnight at room temperature. (c) d-EAK16 was incubated at 100 °C for 4 h, and PBS was added to allow self-assemble for two days. AFM images of d-EAK16 incubated at (d) pH 1, (e) pH 10.6 and (f) pH 12.8 [15]. (Reproduced from Ref. [15] with permission.) For more information, see [21].

20.3.3
A Proposed Model for the Process of Nanofiber Formation

When the peptides form stable β-sheets in water, they form intermolecular hydrogen bonds along the peptide backbones. The β-sheets have two distinct sides, one hydrophobic with an array of alanines and the other with negatively charged aspartic acids and positively charged arginines. On the charged sides, both positive and negative charges are packed together through intermolecular ionic interactions in a checkerboard-like manner. These nanofiber fragments can form various assemblies (Figure 20.6): (a) blunt ends or (b) protruding ends, (c) fragments with semi-protruding ends (only one end "sticky"), or (d) protruding ends (both ends "sticky") readily reassemble through hydrophobic interactions. (e) When the nanofiber fragments first meet, the hydrophobic sides may not fit perfectly but with gaps. However, the non-specific hydrophobic interactions permit the nanofiber

Color Fig.: **20.6**

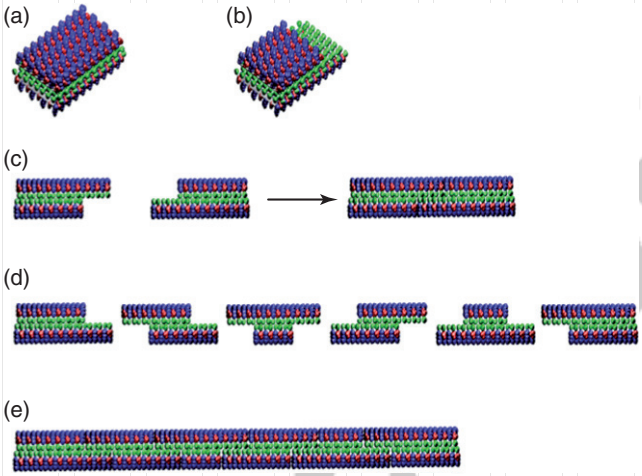

Figure 20.6 A proposed molecular sliding diffusion model for dynamic reassembly of self-assembling RADA16-I peptide. (Image courtesy of Hidenori Yokoi.) Color code: green, alanines; red, negatively charged aspartic acids; blue, positively charged arginines. See text for details. (Reproduced from with permission from Ref. [16].)

to slide-diffuse along the fiber in either direction to minimize the exposure of hydrophobic alanines and eventually fill the gaps [16]. For clarity, these β-sheets are not presented as twisted strands.

20.4 Diverse Applications of Self-Assembling Peptide Nanofibers Scaffolds

20.4.1 Three-Dimensional Tissue Cell Cultures

The ideal biological scaffold and its building blocks must meet several criteria [23]. They should: (i) derive from chemically well defined, synthetic sources from natural building blocks; (ii) be amenable to design and modification to customize specific bioactive and functional requirements; (iii) allow cell attachment, migration, cell–cell, cell–substrate interactions, and recovery of cells from the scaffold; (iv) exhibit non-cytotoxicity, biocompatibility, and be soluble in aqueous solutions, cell culture, and physiological conditions; (v) be optically transparent, compatible with microscopy, flow cytometry, and other analyses; (vi) be sterile and stable for long shelf life, easy transportation, bioproduction, and medically safe for cell therapies; (vii) be economically scalable for affordable material production, purification, and processing; (viii) exhibit a controlled rate of material biodegradation *in vivo* with non-detectable immune responses and non-inflammation; (ix) foster cell migration and angiogenesis to rapidly integrate with tissues in the body; and

Color Fig.: **20.7**

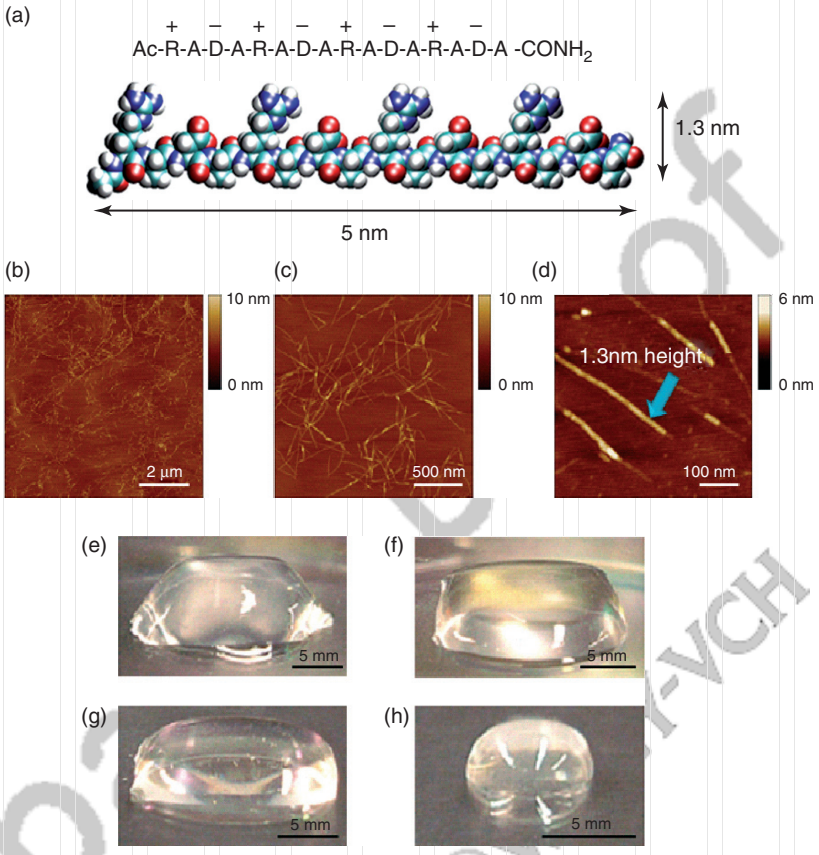

Figure 20.7 Self-assembly of the peptide RADA16-I. (a) Amino acid sequence and molecular model of RADA16-I. AFM images of RADA16-I nanofiber scaffolds. (b) 8 mm^2. (c) 2 mm^2 and (d) 0.5 mm^2. The height of the nanofiber in (d) suggests a double layer structure. Photographs of RADA16-I hydrogel at various conditions. (e) 0.5 wt% (pH 7.5), (f) 0.1 wt% (pH 7.5, Tris. HCl). (g) 0.1 wt% (pH 7.5, PBS) before sonication. (h) re-assembled RADA16-I hydrogel after four times of sonication, respectively. (Image courtesy of Hidenori Yokoi. Reproduced from Ref. [16] with permission.)

(x) be injectable together with cells and compatible with cell delivery and surgical tools.

Biocompatible scaffolds assist in providing a template for cell distribution and ECM accumulation in a 3D geometry. Peptides including RADA16, EAK16, KFE8, KLD12, and d-EAK16, made from L-form and D-form amino acids, undergo self-assembly into well-ordered nanofiber scaffolds. The process of self-assembly into nanofibers is induced by 10 mM NaCl or KCl and occurs over 24 h [21]. These peptides can be designed to incorporate specific ligands, including ECM ligands for cell receptors, chemically synthesized and purified to near homogeneity in kilogram quantities (Figure 20.7).

Since the scaffolds consist of ~99.0–99.5% water with 0.5–1% peptide (Figure 20.7), the storage moduli can be significantly augmented to meet the requirements of the specific research application (cartilage regeneration, stem cell differentiation, etc.). The open network allows cells to migrate freely without hindrance. Because the resulting nanofibers (~10–20 nm, Figures 20.4 and 20.7) are 1000-fold smaller than synthetic polymer microfibers, they can surround cells in a manner similar to the ECM. Moreover, biomolecules in such a nanoscale environment diffuse slowly and are likely to establish a local molecular gradient [24].

Using the nanofibers system, every ingredient of the scaffold can be defined, just as in a two-dimensional Petri dish; the only difference is that cells now reside in a 3D environment where the ECM receptors on the cell surface can bind to the ligands on the peptide scaffold (Figure 20.8b). Cells can now behave and migrate in a truly 3D manner. Beyond the Petri dish, higher tissue architectures with multiple cell types, rather than monolayers, can also be constructed for tissues using the 3D self-assembling peptide scaffolds (Table 20.2).

20.4.2 Cell and Tissue Engineering

Designer self-assembling peptide nanofiber scaffolds have been used to culture diverse types of tissue cells, including stem and progenitor cells, as well as differentiated cell types (Figure 20.8). As early as 1995, we cultured more than 10 mammalian cell stains in scaffolds made of the 2 oligopeptide matrices RAD16 and EAK16, and demonstrated that both the nanoscaffolds can attach to cells [4]. Subsequently, we have used self-assembling peptide monolayers for microcontact printing [11], supported neuronal cell attachment and differentiation, as well as extensive neurite outgrowth (Figure 20.8a) [25], cartilage repairing (Figure 20.8d) [28], created intramyocardial microenvironments for endothelial cells [30], or combined with other biomaterials (RAD16-I and Poly HIPE) on osteoblast proliferation, differentiation, and mineralized matrix formation *in vitro* (Figure 20.8e) [29]. These results illustrate that self-assembling peptides have versatile applications in cell culture. Later Davis *et al.* developed a biotin sandwich method for targeting IGF-1 to self-assembling peptides RAD16-II [30], and Gelain *et al.* attached several functional motifs, including cell adhesion, differentiation, and bone marrow homing motifs, to a self-assembling peptide RAD16 (Figure 20.8b) [26]. VEVK9 and VEVK12 were directly coupled to short biologically active motifs, and significantly stimulated periodontal ligament fibroblasts to produce ECM proteins without using extra additional growth factors [31, 32]. These designer peptide nanofiber scaffolds provide a promising controlled 3D culture system for diverse tissue cells, and are also useful for general cell engineering [31, 33] (Table 20.2).

Color Fig.: **20.8**

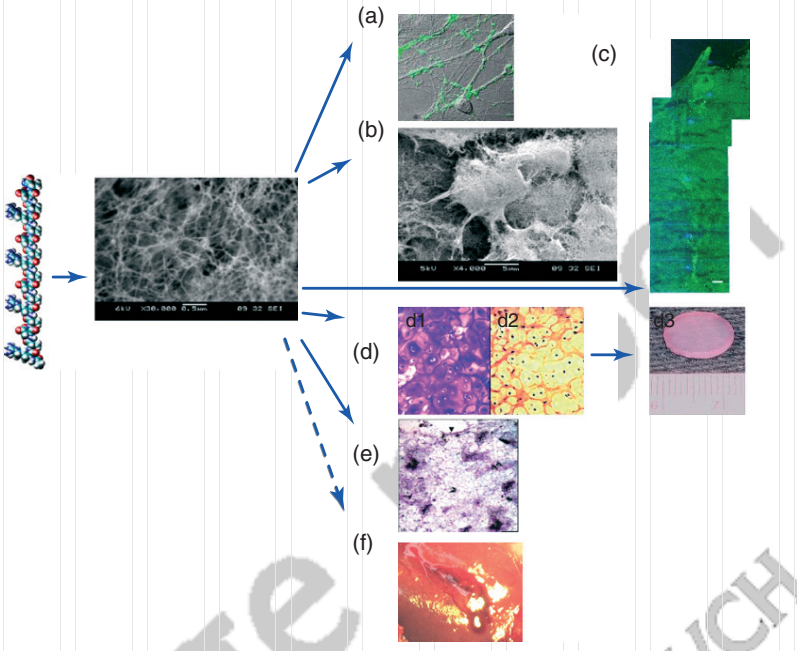

Figure 20.8 From designer peptide to scaffold to tissue engineering [5]. (a) Active synapses on the peptide surface. Primary rat hippocampal neurons form active synapses on peptide scaffolds. The confocal images showed bright discrete green dot labeling indicative of synaptically active membranes after incubation of neurons with the fluorescent lipophilic probe FM-143. FM-143 can selectively trace synaptic vesicle turnover during the process of synaptic transmission. The active synapses on the peptide scaffold are fully functional, indicating that the peptide scaffold is a permissible material for neurite outgrowth and active synapse formation. (Reproduced from Ref. [25] with permission.) (b) Adult mouse neural stem cells embedded in 3D scaffold. (Reproduced from Ref. [26] with permission.) (c) Brain damage repair in hamster. The peptide scaffold was injected into the optical nerve area of brain that was first severed with a knife. The gap was sealed by the migrating cells after a few days. A great number of neurons form synapses. (Reproduced from Ref. [27] with permission.) (d) Peptide KLD12 (KLDLKLDLKLDL), chondrocytes in the peptide scaffold and cartilage. The chondrocytes stained with TB showing abundant GAG production (d1) and antibody to type II collagen demonstrating abundant Type II collagen production (d2). A 12-mm chondrocyte-seeded peptide hydrogel plug, punched from 1.6-mm-thick slabs (d3). The cartilage formed over a three to four week period after the initial seeding of the chondrocytes. (Reproduced from Ref. [28] with permission.) (e) Von Kossa staining showing transverse sections of primary osteoblast cells on HA-PHP-RADA16-I self-assembling peptide nanofiber scaffold. Scale bar = 0.1 mm. The intensely stained black areas represent bone nodules forming. (Reproduced from Ref. [29] with permission.) (f) Tests of rabbit liver hemostasis *in situ*. The optical microscopy images of rabbit liver cut are added to d-EAK16 solution. The rapid hemostasis is ~20 s. (Reproduced from Ref. [21] with permission.)

Table 20.2 Some typical self-assembling peptides and their applications[a].

Name	Sequence	Applications[c]
EAK16	AcN-AEAEAKAKAEAEAKAK-CNH_2	Cell culture; drug delivery
RAD16-I or RADA16	AcN-RADARADARADARADA-CNH_2	Neurite outgrowth; repair injured brain; second degree burns; drug delivery
RAD16-II	AcN-RARADADARARADADA-CNH_2	Cell culture
KLD12	AcN-KLDLKLDLKLDL-CNH2	Cartilage repair
VEVK9	Ac-VEVKVEVKV-CNH2	Cell culture
d-EAK16	AcN$(-{}^{D}A{}^{D}E{}^{D}A{}^{D}E{}^{D}A{}^{D}K{}^{D}A{}^{D}K)_2$-$CNH_2$	Cell culture; trauma emergency

[a]All these peptides form nanofibers that self-assembled in PBS buffer.

20.4.3 Controlled Drug Delivery and Regenerative Medicine

The characteristic features of self-assembling peptides (alternating hydrophobic and hydrophilic residues and distinct periodicity of polar and non-polar, negative and positive charge distribution) promote their use in drug delivery [5]. Chen and coworkers used EAK16-II to encapsulate the extremely hydrophobic compound pyrene [34]. Encapsulated pyrene adopts a crystalline form but is slowly released with a time profile following a single exponential decay. Higher peptide-to-pyrene ratios lead to slower transfer of pyrene to the lipophilic environment. Similar conclusions were drawn by Zhao and coworkers using the ionic complementary peptides RAD16-II [35] and RAD16-I [36]. Studies on chemical dye molecules like Phenol Red, Bromophenol Blue, 8-hydroxypyrene-1,3,6-trisulfonic acid trisodium salt (pyranine, 3-PSA), 1,3,6,8-pyrenetetrasulfonic acid tetrasodium salt (4-PSA), and Coomassie Brilliant Blue G-250 (CBBG) showed that they interact strongly with the RAD16-I peptide scaffolds and the diffusivities of the dyes decreased with increasing hydrogel peptide concentration. Self-assembling peptides can also control the release of some small protein macromolecules, like lysozyme, trypsin inhibitor, BSA, and a monoclonal IgG antibody [24]. Importantly, encapsulation and release did not affect the protein conformation and functionality, the enzyme still catalyzed its substrate and the monoclonal antibody still bound its antigen well. In addition, the RAD16-I scaffolds facilitate slow and sustained release of active cytokines like βFGF, VEGF, and BDNF [37]. The results not only provide evidence for long-term molecular release from self-assembling peptide scaffolds but also inspire a plethora of slow molecular release strategies for clinical applications.

Ellis-Behnke *et al.* used self-assembling peptide RAD16-I to repair injured brain structures (Figure 20.8c) [27]. The result showed the peptide nanofibers not only regenerate axons at the site of injury but also knit the brain tissue together. Zhao and his colleagues also used the same peptide to repair deep second degree burns in rats [38]. RAD16-I can advance the time of both eschar appearance and

disappearance by three to five days, and speed up wound contraction by 20–30% compared with other groups (treated with chitosan, PLA, collagen I, or blank) without obvious edema. Immunohistochemical studies showed that both FGF and EGF were expressed in nascent tissue such as epidermis and glands when wounds were treated with RADA16-I after injury [38]. The self-assembling peptide consists of ~99.0–99.5% water and supports cell adhesion, migration, and differentiation. This may be a promising burn wound dressing which is simple, effective, and affordable (Table 20.2).

20.4.4 Trauma Emergency

Ellis-Behnke *et al.* found that self-assembling peptide RAD16-I stopped bleeding quickly during the procedure of repairing injured rat brains. This principle could be extended to the spinal cord, femoral artery, and liver [39]. In 2009, Zhao and his colleagues utilized an injury model to evaluate the hemostatic efficacy of peptide RAD16-I in rat kidney [40]. We have elucidated the basis for this ability to induce rapid hemostasis. Using D-amino acids, the chiral self-assembling peptide d-EAK16 also forms a 3D nanofiber scaffold that is indistinguishable from its counterpart l-EAK16 [21]. These chiral peptides containing all D-amino acids, d-EAK16 self-assemble into well-ordered nanofibers. However, peptides with alternating D- and L-amino acids, EA*K16 and E*AK*16 showed poor self-assembling properties [20]. 1% (w/w) d-EAK16 took ~20 s to induce liver wound hemostasis, but 1% (w/w) of E*A*K16 and EA*K16 that have alternating chiral D- and L-amino acids took ~70 and ~80 s, respectively (Figure. 20.8f). We have proposed a model named "nano-fishnet rapid hemostasis" not only to provide insights in understanding the chiral assembly properties for rapid hemostasis, but also to aid in further design of self-assembling D-form peptide scaffolds for clinical trauma emergency [21] (Table 20.2).

Recent advances in functionalization have also led to the development of better synthetic tissue cell culture bioactive scaffolds that promote cell proliferation, migration, and differentiation for regenerative medicine. Several non-functionalized self-assembling peptide scaffolds are already in clinical trial. It is our hope that in the not too distant future, they will open the door for more clinical applications in biomedicine.

20.5 Summary

Designed D- and L-chiral self-assembling peptides undergo major conformational transformations in response to changes in temperature and pH. Since the unexpected discovery of the self-assembling peptide EAK16-II in the yeast protein *Zuotin*, we have come a long way in understanding not only the design principles at the molecular level, the molecular and ultra-fine material structures, interactions of

the peptides, the dynamic self-assembly behavior, but also how to further improve their design for delivering bioactive therapeutics such as drugs and growth factors, and monoclonal antibodies. We have expanded the range of self-assembling designer materials using natural L-amino acids and chiral form D-amino acids. We have developed various applications in many areas including (i) 3D tissue cell cultures, (ii) cell and tissue engineering, (iii) controlled and sustained molecular delivery and regenerative medicine, and (iv) trauma emergency. With many and more people becoming interested in self-assembling peptides, there will likely be many more surprising applications in the years to come.

Acknowledgments

ZL was supported in part by China National ''985 Project'' and by the grant from the Natural Science Foundation Project of CQ CSTC (2011BB5134), Specialized Research Fund for the Doctoral Program of Higher Education (20115503120010), and National Natural Science Foundation of China (NSFC,81101417). We thank the editor for critical reading and helpful discussions.

References

1. Zhang, S. (2003) Fabrication of novel biomaterials through molecular self-assembly. *Nat. Biotechnol.*, **21**, 1171–1178.
2. Zhang, S., Holmes, T., Lockshin, C., and Rich, A. (1993) Spontaneous assembly of a self-complementary oligopeptide to form a stable macroscopic membrane. *Proc. Natl. Acad. Sci. U.S.A.*, **90**, 3334–3338.
3. Zhang, S. (2002) Emerging biological materials through molecular self-assembly. *Biotechnol. Adv.*, **20**, 321–339.
4. Zhang, S., Holmes, T., DiPersio, M., Hynes, R.O., Su, X., and Rich, A. (1995) Self-complementary oligopeptide matrices support mammalian cell attachment. *Biomaterials*, **16**, 1385–1393.
5. Hauser, C.A.E. and Zhang, S. (2010) Designer self-assembling peptide nanofiber biological materials. *Chem. Soc. Rev.*, **39**, 2780–2790.
6. Zhang, S. and Rich, A. (1997) Direct conversion of an oligopeptide from a beta-sheet to an alpha-helix: a model for amyloid formation. *Proc. Natl. Acad. Sci. U.S.A.*, **94**, 23–28.
7. Xiong, H., Buckwalter, B.L., Shieh, H.M., and Hecht, M.H. (1995) Periodicity of polar and nonpolar amino acids is the major determinant of secondary structure in self-assembling oligomeric peptides. *Proc. Natl. Acad. Sci. U.S.A.*, **92**, 6349–6353.
8. Cerpa, R., Cohen, F.E., and Kuntz, I.D. (1996) Conformational switching in designed peptides: the helix/sheet transition. *Fold. Des.*, **1**, 91–101.
9. Rippon, W.B., Chen, H.H., and Walton, A.G. (1973) Spectroscopic characterization of poly(Glu-Ala). *J. Mol. Biol.*, **75**, 369–375.
10. Aggeli, A., Nyrkova, I.A., Bell, M., Harding, R., Carrick, L., McLeish, T.C.B., Semenov, A.N., and Boden, N. (2001) Hierarchical self-assembly of chiral rod-like molecules as a model for peptide β-sheet tapes, ribbons, fibrils, and fibers. *Proc. Natl. Acad. Sci. U.S.A.*, **98**, 11857–11862.
11. Zhang, S., Yan, L., Altman, M., Lässle, M., Nugent, H., Frankel, F., Lauffenburger, D.A., Whitesides, G.M., and Rich, A. (1999) Biological surface engineering: a simple system for cell pattern formation. *Biomaterials*, **20**, 1213–1220.

12. Kirschner, D.A., Inouye, H., Duffy, L.K., Sinclair, A., Lind, M., and Selkoe, D.J. (1987) Synthetic peptide homologous to beta protein from Alzheimer disease forms amyloid-like fibrils in vitro. *Proc. Natl. Acad. Sci. U.S.A.*, **84**, 6953–6957.
13. Harper, J.D., Lieber, C.M., and Lansbury, P.T. (1997) Atomic force microscopic imaging of seeded fibril formation and fibril branching by the Alzheimer's disease amyloid-beta protein. *Chem. Biol.*, **4**, 951–959.
14. Altman, M., Lee, P., Rich, A., and Zhang, S. (2000) Conformational behavior of ionic self-complementary peptides. *Protein Sci.*, **9**, 1095–1105.
15. Luo, Z., Zhao, X., and Zhang, S. (2008) Structural dynamic of a self-assembling peptide d-EAK16 made of only D-amino acids. *PLoS ONE*, **3**, e2364.
16. Yokoi, H., Kinoshita, T., and Zhang, S. (2005) Dynamic reassembly of peptide RADA16 nanofiber scaffold. *Proc. Natl. Acad. Sci. U.S.A.*, **102**, 8414–8419.
17. Macfarlane, R.G. (1964) An enzyme cascade in the blood clotting mechanism and its function as a biochemical amplifier. *Nature*, **202**, 498–499.
18. Barrow, C.J. and Zagorski, M.G. (1991) Solution structures of beta peptide and its constituent fragments: Relation to amyloid deposition. *Science*, **253**, 179–182.
19. Mutter, M., Gassmann, R., Buttkus, U., and Altmann, K.H. (1991) Switch peptides: pH-induced α-helix to β-sheet transitions of bis-amphiphilic oligopeptides. *Angew. Chem. Int. Ed. Engl.*, **30**, 1514–1516.
20. Marqusee, S. and Baldwin, R.L. (1987) Helix stabilization by Glu-. . . Lys+ salt bridges in short peptides of de novo design. *Proc. Natl. Acad. Sci. U.S.A.*, **84**, 8898–8902.
21. Luo, Z., Wang, S., and Zhang, S. (2011) Fabrication of self-assembling D-form peptide nanofiber scaffold d-EAK16 for rapid hemostasis. *Biomaterials*, **32**, 2013–2020.
22. Luo, Z., Zhao, X., and Zhang, S. (2008) Self-organization of a chiral D-EAK16 designer peptide into a 3D nanofiber scaffold. *Macromol. Biosci.*, **8**, 785–791.
23. Zhang, S., Zhao, X., and Spirio, L. (2006) *Scaffolding in Tissue Engineering*, Taylor & Francis Group, LLC.
24. Koutsopoulos, S., Unsworth, L.D., Nagai, Y., and Zhang, S. (2009) Controlled release of functional proteins through designer self-assembling peptide nanofiber hydrogel scaffold. *Proc. Natl. Acad. Sci. U.S.A.*, **106**, 4623–4628.
25. Holmes, T.C., de Lacalle, S., Su, X., Liu, G., Rich, A., and Zhang, S. (2000) Extensive neurite outgrowth and active synapse formation on self-assembling peptide scaffolds. *Proc. Natl. Acad. Sci. U.S.A.*, **97**, 6728–6733.
26. Gelain, F., Lomander, A., Vescovi, A.L., and Zhang, S. (2006) Designer self-assembling peptide nanofiber scaffolds for adult mouse neural stem cell 3-dimensional cultures. *PLoS ONE*, **1**, e119.
27. Ellis-Behnke, R.G., Liang, Y.-X., You, S.-W., Tay, D.K.C., Zhang, S., So, K.-F., and Schneider, G.E. (2006) Nano neuro knitting: peptide nanofiber scaffold for brain repair and axon regeneration with functional return of vision. *Proc. Natl. Acad. Sci. U.S.A.*, **103**, 5054–5059.
28. Kisiday, J., Jin, M., Kurz, B., Hung, H., Semino, C., Zhang, S., and Grodzinsky, A.J. (2002) Self-assembling peptide hydrogel fosters chondrocyte extracellular matrix production and cell division: Implications for cartilage tissue repair. *Proc. Natl. Acad. Sci. U.S.A.*, **99**, 9996–10001.
29. Bokhari, M.A., Akay, G., Zhang, S., and Birch, M.A. (2005) The enhancement of osteoblast growth and differentiation in vitro on a peptide hydrogel—polyHIPE polymer hybrid material. *Biomaterials*, **25**, 5198–5208.
30. Davis, M.E., Motion, J.P.M., Narmoneva, D.A., Takahashi, T., Hakuno, D., Kamm, R.D., Zhang, S., and Lee, R.T. (2005) Injectable self-assembling peptide nanofibers create intramyocardial microenvironments for endothelial cells. *Circulation*, **111**, 442–450.
31. Kumada, Y., Hammond, N.A., and Zhang, S. (2010) Functionalized scaffolds of shorter self-assembling peptides containing MMP-2 cleavable motif promote fibroblast proliferation and

significantly accelerate 3-D cell migration independent of scaffold stiffness. *Soft Matter*, **6**, 5073–5079.

32. Kumada, Y. and Zhang, S. (2010) Significant type I and type III collagen production from human periodontal ligament fibroblasts in 3D peptide scaffolds without extra growth factors. *PLoS ONE*, **5**, e10305.

33. Wang, X., Horii, A., and Zhang, S. (2008) Designer functionalized self-assembling peptide nanofiber scaffolds for growth, migration, and tubulogenesis of human umbilical vein endothelial cells. *Soft Matter*, **4**, 2388–2395.

34. Keyes-Baig, C., Duhamel, J., Fung, S.-Y., Bezaire, J., and Chen, P. (2004) Self-assembling peptide as a potential carrier of hydrophobic compounds. *J. Am. Chem. Soc.*, **126**, 7522–7532.

35. Li, F., Wang, J., Tang, F., Lin, J., Zhang, Y., Zhang, E.-Y., Wei, C., Shi, Y.-K., and Zhao, X. (2009) Fluorescence studies on a designed self-assembling peptide of RAD16-II as a potential carrier for hydrophobic drug. *J. Nanosci. Nanotechnol.*, **9**, 1611–1614.

36. Tang, F. and Zhao, X. (2010) Interaction between a self-assembling peptide and hydrophobic compounds. *J. Biomater. Sci. Polym. Ed.*, **21**, 677–690.

37. Gelain, F., Unsworthb, L.D., and Zhang, S. (2010) Slow and sustained release of active cytokines from self-assembling peptide scaffolds. *J. Control. Release*, **145**, 231–239.

38. Meng, H., Chen, L., Ye, Z., Wang, S., and Zhao, X. (2008) The effect of a self-assembling peptide nanofiber scaffold (Peptide) when used as a wound dressing for the treatment of deep second degree burns in rats. *J. Biomed. Mater. Res. B Appl. Biomater.*, **89B**, 379–391.

39. Ellis-Behnke, R.G., Liang, Y.-X., Tay, D.K.C., Kau, P.W.F., Schneider, G.E., Zhang, S., Wu, W., and So, K.-F. (2006) Nano hemostat solution:immediate hemostasis at the nanoscale. *Nanomedicine*, **2**, 207–215.

40. Song, H., Zhang, L., and Zhao, X. (2009) Hemostatic efficacy of biological self-assembling peptide nanofibers in a rat kidney model. *Macromol. Biosci.*, **10**, 33–39.

''keywords/abstract

Dear Author,

Keywords and abstracts will not be included in the print version of your chapter but only in the online version. Please check and/or supply keywords. If you supplied an abstract with the manuscript, please check the typeset version. If you did not provide an abstract, the section headings will be displayed instead of an abstract text in the online version.

Thank you!''

Abstract

Keywords
Alzheimer's disease; β-amyloid; self-assembling peptides; α-helices; β-sheets

Affiliation for the Authors: Zhongli Luo[1,2] and Shuguang Zhang[2]
[1]Chongqing Medical University, College of Basic Medical Sciences, Molecular Medicine and Cancer Research Center, Chongqing, China
[2]Massachusetts Institute of Technology, Laboratory for Molecular Design, Center for Bits and Atoms, 77 Massachusetts Avenue, Cambridge, MA, 02139-4307, USA

Queries in Chapter 20

Q1. Please give full address, i.e., street name

Q2. Please provide the explanation for the footnote indicator "c" in Table 20.1.